Numerical Study of Heat Transfer from an Isothermal Vertical Plate in an Air Enclosure

S. A. Ayo

Department of Mechanical Engineering,
Federal University of Technology,Minna, Nigeria.
e-mail: sa_ayo@yahoo.com

Abstract

The numerical study of the heat transfer from an isothermal vertical plate in an air enclosure is undertaken in this work to simulate heat transfer from electronic elements and similar devices as functions of plate locations and Grashof number. The walls of the enclosure are assumed to be adiabatic and the full two-dimensional time-dependent partial differential forms of the conservation equations of continuity, momentum, and energy governing the flow field are cast and solved by a numerical method employing the finite-difference scheme. During the initial short period, heat flow is found to be by conduction irrespective of plate location and Grashof number. Shortly after conduction sets in convection indicated by increase in the heat transfer coefficient following a temporal minimum in the coefficient at the end of the conduction regime. Heat transfer by convection is found to be maximum when the plate is symmetrically located within the enclosure, the rate decreasing as the plate is moved away from this location along a horizontal direction. It is also found that there is very little change in the heat transfer rate when the plate is moved downwards from the centre of the enclosure along the vertical direction, indicated by the collinearity of the curves along the direction, but a sharp decrease occurs when the plate is moved upwards along the axis. During convection the rate of heat transfer is found to increase with Grashof number. For low Grashof numbers, e.g. for H/L=1/4 and Gr = 4650, and for H/L=1/4 and Gr = 46500, the regime of heat transfer is found to be entirely the one-dimensional conduction regime. At large times the temperature field stratifies and heat transfer from the heated surface into the fluid medium approaches zero, the velocity field decaying gradually and the flow approaching its eventual quiescence.

I   INTRODUCTION

The study of natural convection has become very important because of its wide range of occurrence and the role it plays in enhancing the performance of most thermal equipment. And specifically, the study of natural convection in enclosures has been of necessity because of the growing number of areas of application. It is very widely utilized in the electronics industry as the mode of cooling for the high energy dissipating elements such as circuit boards or cards of electronic devices. In nuclear industry, it is utilized for cooling reactor cores during power or pump failures. Although a lot of methods for cooling these devices have been adopted the method of natural convection still remains the simplest, cheap, most reliable, maintenance-free, quiet, and safe technique. Other areas of application include residential heating, and more recently, solar energy field, and thermal storage systems. In these areas, convection has served as one of the principal modes of transfering energy for some useful heating purposes.

Khalilolahi & Sammakia (1986) used the simple arbitrary Langrangian-Eulerian (SALE) technique to analyze the full two-dimensional equations representing mass, momentum, and energy balance for unsteady buoyancy-induced flow generated by an isothermal vertical surface enclosed in a long rectangular cavity. He considered

the plate to be centrally located and used symmetry to analyze the flow for one-half of the enclosure. He observed the quasi-one-dimensional conduction regime adjacent to the surface at very short times, the steady boundary-layer flow near a semi-infinite surface in an infinite media at intermediate times, and at later times, stratification of temperature field as flow approaches its eventual quiescence. Eseki et al (1993) studied the cases of flow generated by an isothermal vertical surface and one with constant heat flux in a square cavity with the base adiabatic and other walls at a constant cold temperature. He discovered that for the case of the isothermal surface, the heat flux on the opposite side of the hot surface increases when the surface is moved from a position very close to the left side vertical bounding walls towards the vertical line of symmetry of the plate and the rate decreases as the line of symmetry is approached. The same result was observed at the right side bounding walls. He further reported that for a vertical shift of the plate, for high Ra, (Ra $\geq$ 3 x 10^6) the maximum heat transfer rate occurs when the plate is located at one-third of the height of the cavity, for Ra about 10^6 only small changes in the heat transfer rate occurs, and for lower Ra. (Ra. $\leq 10^6$) significant changes in the rate of heat transfer are introduced, with the maximum occurring closer to the top of the cavity.

Sammakia et al (1980) conducted both experimental and analytical (numerical) investigation on transient natural convection generated by a semi-infinite surface in air and in water, and the results from the two showed close agreement especially for the laminar flow regime. Hellums and Churchill (1962) used an explicit finite-difference scheme to solve the full boundary layer equations in their time-dependent partial differential forms representing the flow field adjacent to a semi-infinite flat vertical isothermal surface in an infinite medium. The results were in excellent agreement with the early analysis due to Ostrach (1972).

Also, the results for measurements by Gebhart and Adams (1962) agree well with those of the integral method of Gebhart (1961) in the analysis of transients adjacent to a semi-infinite vertical plate.

The present work focuses on heat transfer from an isothermal vertical plate in an air enclosure. Motivation for this study has been aroused by the observed early heat accumulation tendencies of electronic components in sealed enclosures, which could have adverse effect on the performance of the devices. The research seeks to investigate the various regimes of heat transfer and their characteristics, and the rates of heat transfer, defined in quantitative terms, from the surfaces as functions of plate location and the Grashof number which is a measure of the temperature difference between the heated plate and the fluid medium. In the study, the full two-dimensional conservation equations governing the flow field are numerically analyzed assuming adiabatic conditions.

II   MATHEMATICAL FORMULATION

The physical problem is modelled as a two-dimensional rectangular enclosure with adiabatic walls on all sides, filled with air (see figure 1) below. The source of heat, the vertical plate, is an isothermal element of negligible thickness which is moved around within the enclosure in a vertical orientation. At the initial time, the fluid, the plate, and the bounding walls are all at the same initial ambient temperature, T_i, until suddenly the temperature of the plate is raised and maintained at a higher, uniform and constant value, T_w.

The following assumptions are made in order to simplify the analysis of the problem:

(i)   The flow is laminar and two-dimensional

(ii)   .The fluid is Newtonian, viscous, and incompressible

(iii)   Fluid properties are constant except in the buoyancy term consideration
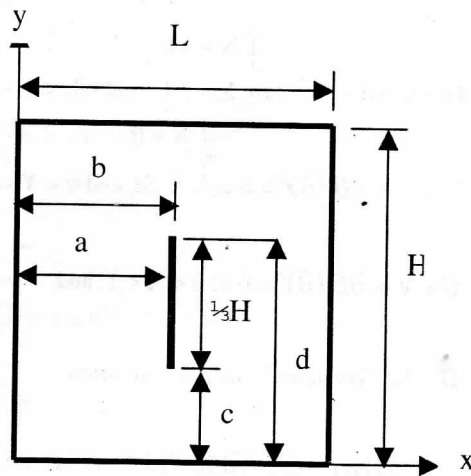
(iv)   Viscous dissipation term is negligible

Figure 1. The physical model

(v) Heat flow by radiation is negligible

(vi) No internal heat source or heat sink is

(vii) involved

(viii) The walls are impermeable and the no-slip condition applies.

The appropriate equations governing the flow field are the conservation equations of mass, momentum, and energy;

$$\frac{\partial u}{\partial x} + \frac{\partial v}{\partial y} = 0 \qquad (1)$$

$$\frac{\partial u}{\partial t} + u\frac{\partial u}{\partial x} + v\frac{\partial u}{\partial y} = -\frac{1}{\rho}\frac{\partial p}{\partial x} + v\nabla^2 u \qquad (2)$$

$$\frac{\partial v}{\partial t} + u\frac{\partial v}{\partial x} + v\frac{\partial v}{\partial y} = -\frac{1}{\rho}\frac{\partial p}{\partial y} + v\nabla^2 v + F_y \qquad (3)$$

$$\frac{\partial T}{\partial t} + u\frac{\partial T}{\partial x} + v\frac{\partial T}{\partial y} = \alpha\nabla^2 T \qquad (4)$$

where, u is horizontal component of velocity

v is vertical component of velocity

T is temperature

t is time

y is vertical coordinate

x is horizontal component

ρ is density of fluid inside the heated layer

p is pressure

v is the kinematic viscosity of the fluid

α is the thermal diffusivity

The body force due to buoyancy in the y-direction can be obtained by the Boussisesqu approximation,

$$\rho = \rho_o (1 + \beta\Delta T) \qquad (5)$$

where, β is the volume coefficient of thermal expansion

ρ_o is the bulk fluid density,

ΔT is the temperature difference between the heated layer and the bulk value,

The body force per unit mass, F_y, due to buoyancy in the y-direction is obtained thus,

$$F_y = -\beta g (\Delta T)$$

where, g is the acceleration due to gravity.

The y-momentum equation becomes,

$$\frac{\partial v}{\partial t} + u\frac{\partial v}{\partial x} + v\frac{\partial v}{\partial y} = -\frac{1}{\rho}\frac{\partial p}{\partial y} + v\nabla^2 v - \beta g (\Delta T) \qquad (6)$$

A Boundary and Initial Conditions

The above governing equations are subject to the following initial and boundary conditions:

at t = 0, $u = v = T - T_i = 0$,

for t > 0,

$u = v = T - T_w = 0$ at $\begin{cases} x = a \\ x = b, \quad \text{and } c < y < d, \end{cases}$

$u = v = \partial T / \partial x = 0$ at $\begin{cases} x = 0 \\ x = L, \text{ and } 0 < y < H \end{cases}$

$u = v = \partial T / \partial y = 0$ at $0 < x < L$ and $\begin{cases} y = 0 \\ y = H \end{cases}$

B Normalization of the Governing Equations

Following Khalilolahi and Sammakia (1986), the equations are made dimensionless for generalization using the following non-dimensionalizing parameters:

$X = x/L; \ Y = y/L; \ U = uL/v; \ V = vL/v; \ \tau = tv/L^2$

181

$$\theta = (T - T_i)/(T_w - T_i); \quad P = PL^2/\rho v^2$$

where, Y is dimensionless vertical coordinate

X is dimensionless horizontal coordinate

U is dimensionless horizontal component of velocity

V is dimensionless vertical component of velocity

T_i is initial temperature

T_w is temperature of isothermal wall

θ is dimensionless temperature

τ is dimensionless time

p is dimensionless pressure

The dimensionless form of the equations and the boundary and initial conditions are thus as follows:

$$\frac{\partial U}{\partial X} + \frac{\partial V}{\partial Y} = 0 \qquad (7)$$

$$\frac{\partial U}{\partial \tau} + U\frac{\partial U}{\partial X} + V\frac{\partial U}{\partial Y} = -\frac{\partial P}{\partial X} + \frac{\partial^2 U}{\partial X^2} + \frac{\partial^2 U}{\partial Y^2} \qquad (8)$$

$$\frac{\partial V}{\partial \tau} + U\frac{\partial V}{\partial X} + V\frac{\partial V}{\partial Y} = -\frac{\partial P}{\partial Y} + \frac{\partial^2 V}{\partial X^2} + \frac{\partial^2 V}{\partial Y^2} + Gr\theta ..(9)$$

$$\frac{\partial \theta}{\partial \tau} + U\frac{\partial \theta}{\partial X} + V\frac{\partial \theta}{\partial Y} = \frac{1}{Pr}\left(\frac{\partial^2 \theta}{\partial X^2} + \frac{\partial^2 \theta}{\partial Y^2}\right) \qquad (10)$$

where, $Gr = g\beta(T_w - T_i)L^3/v^2$

$Pr = c_p\mu/k$

β is volume coefficient of thermal expansion

c_p is specific heat at constant pressure

μ is dynamic viscosity of fluid

k is thermal conductivity

C. Dimensionless Boundary and Initial Conditions

The normalized boundary and initial conditions are:

at $\tau = 0$, $\quad U = V = \theta = 0$,

for $\tau > 0$,

$$U = V = \theta - 1 = 0 \text{ at} \begin{cases} X = a/L \\ X = b/L, \text{ and } c/L < Y < d/L \end{cases}$$

$$U = V = \partial\theta/\partial Y = 0 \text{ at} \begin{cases} X = 0 \\ X = 1 \text{ and } 0 < Y < H/L \end{cases}$$

$$U = V = \partial\theta/\partial Y = 0 \text{ at } 0 < X < 1, \text{ and} \begin{cases} Y = 0 \\ Y = H/L \end{cases}$$

D. The Vorticity Transport Equation

The normalized X- and Y- momentum equations are combined together to eliminate the pressure terms, to yield the normalized vorticity transport equation given as,

$$\frac{\partial \omega}{\partial \tau} + U\frac{\partial \omega}{\partial X} + V\frac{\partial \omega}{\partial Y} = \frac{\partial^2 \omega}{\partial X^2} + \frac{\partial^2 \omega}{\partial Y^2} + Gr\frac{\partial \theta}{\partial X} \qquad (11)$$

where, ω is dimensionless vorticity

E. The Poisson Equation for Stream Function

The vorticity transport equation above does not have any explicit boundary conditions for evaluating the vorticities. To solve the problem therefore, the Poisson equation for the stream function, and the velocity-stream function equations are introduced as a means of determining the vorticities at the boundaries. The approach also enables the values of the streamlines within the domain to be generated. The normalized form of the equations conforming with the normalized parameters above are as given below:

$$\frac{\partial^2 \psi}{\partial X^2} + \frac{\partial^2 \psi}{\partial Y^2} = -\omega \qquad (12)$$

$$\frac{\partial \psi}{\partial Y} = U \qquad (13a);$$

$$\frac{\partial \psi}{\partial X} = -V \qquad (13b)$$

subject to the following dimensionless initial and boundary conditions:

at $\tau = 0$, $\quad \omega = \psi = 0$,

for $\tau > 0$,

$$\psi = 0 \text{ at } \begin{cases} X = a/L \\ X = b/L, \text{ and } c/L < Y < d/L, \end{cases}$$

$$\text{at } \begin{cases} X = 0 \\ X = 1 \text{ and } 0 < Y < H/L \end{cases}$$

$$\text{at } 0 < X < 1, \text{ and } \begin{cases} Y = 0 \\ Y = H/L \end{cases}$$

where, ψ is dimensionless stream function

F. Vorticity Boundary Conditions

Following (Shoichiro 1977) the vorticities at the walls are obtained by expanding the stream function values at points adjacent to the walls in the Taylor's series about the walls. After necessary simplifications, the boundary vorticities are approximated by,

$$\omega_{wall} = -\frac{2}{\Delta n^2}\left(\psi_{wall+\Delta n}\right)$$

Δn is a subdivision (ΔX or ΔY) on the axis normal to the surface, taken from the surface into the fluid medium.

At the sharp concave corners, 'b', 'd', 'f', and 'h',

$$\frac{\partial V}{\partial X} = 0 ; \quad \frac{\partial U}{\partial Y} = 0$$

so that at the corners the vorticities vanish, i.e.,

$$\omega_b = \omega_d = \omega_f = \omega_h = 0$$

III   NUMERICAL METHOD OF SOLUTION

The numerical method adopted for solving the system of partial differential equations is the finite difference. The entire domain is subdivided into a mesh system, size m x n, with uniform divisions, ΔX and ΔY, in the X- and Y-directions respectively, ensuring that the boundaries lie on grid points. Because of the derivative boundary conditions, four fictitious lines, two horizontal, distance ΔY top and bottom of the cavity, and two vertical, distance ΔX left and right of the cavity are introduced.

The appropriate finite-difference scheme representations of the partial differential terms in the governing equations are cast and used to replace each of the terms, the central difference approximation being used in the space derivatives, and the forward difference in the time derivatives. Equations (10), (11) and (13) are expressed explicitly, and equation 12 implicitly. The system of discretized equations are then solved numerically starting from time $\tau = 0$, and marched in time, using a sufficiently small time step ($\Delta\tau = 2E-6$) that allows for the stability of the solution, until a desired time is reached. The Von Neumann stability analysis is used in determining the stability criteria.

The system of equations (10), (11), (12), and (13) are solved following a cyclical sequence. During any one time step, the energy transport equation, equation (10), is solved first for θ using the initial values of U, V, and θ. In the next stage and for the same time step, the vorticity transport equation , equation (11), is solved for ω at the interior of the domain, still using the same initial values of U and V but the new values of θ obtained from the solution of equation 10, leaving the vorticities at the boundaries. These most recent values of ω are used in the Poisson equation for stream function, equation (12), to yield a system of simultaneous equations which is now solved for by an iterative scheme to obtain the values of ψ still for the same time step. The vorticities at the boundaries are then evaluated using the values of ψ at the adjacent nodal points perpendicular to the surface. And lastly the X- and Y-velocity equations, equations (13a) & (13b), are solved using the values ψ obtained at the last stages. This completes the first cycle of operations for the first time step. For the second cycle, the values obtained in the first cycle are used to repeat the entire operations again to obtain new distributions for θ, ω, ψ, etc. This operation is repeated until the desired time is reached.

The iterative scheme adopted for solving the implicit stream function equation is the Liebmann iterative method

183

accelerated by the Successive Over-relaxation, (S.O.R), method for convergence. Following Chow (1979) the convergence of the stream function equation is subject to the criterion,

$$\sum_{i=2}^{m}\sum_{j=2}^{n}\left|\psi_{i,j}^{t+1}-\psi_{i,j}^{t}\right|\leq\delta$$

where, δ is the residue taken as 1×10^{-04}

A. Heat Transfer Calculation

The effect of fluid motion on the rate of heat transfer from the hot surface into the fluid medium is expressed in terms of Nusselt numbers. The Nusselt number is evaluated at specific points as local Nusselt number, or averaged over one of the plate surfaces as local mean Nusselt number, or over the entire surface as overall mean Nusselt number.

The local mean Nusselt numbers at the sides, and bottom and top of the plate are therefore expressed respectively as,

$$Nu=-\frac{\partial\theta}{\partial X}; \quad Nu=-\frac{\partial\theta}{\partial Y}$$

And the overall mean Nusselt number is expressed as

$$\overline{Nu}=\frac{\left(\overline{Nu_R}+\overline{Nu_L}\right)\left(d_j-c_j+1\right)+\left(\overline{Nu_B}+\overline{Nu_T}\right)\left(b_i-a_i+1\right)}{2\left(d_j-c_j+1\right)\left(b_i-a_i+1\right)}$$

Where, a_i and b_i, and c_j and d_j are respectively the X- and Y-coordinates of the corners of the plate. Nu_L and Nu_R are respectively the mean Nusselt numbers at the left and right sides of the plate, while Nu_T and Nu_B are respectively the mean Nusselt numbers at the top and bottom of the plate expressed as

$$\overline{Nu_L}=-\frac{1}{L_p}\int_{c_j}^{d_j}\frac{\partial\theta}{\partial X}dY\Big|_{x=n}$$

$$\overline{Nu_R}=-\frac{1}{L_p}\int_{c_j}^{d_j}\frac{\partial\theta}{\partial X}dY\Big|_{x=b}$$

$$\overline{Nu_T}=-\frac{1}{B_p}\int_{a_j}^{h_j}\frac{\partial\theta}{\partial Y}dX\Big|_{Y=d}$$

$$\overline{Nu_B}=-\frac{1}{B_p}\int_{a_j}^{h_j}\frac{\partial\theta}{\partial Y}dX\Big|_{Y=c}$$

$$L_p=d-c; \quad B_p=b-a$$

The mean Nusselt numbers are evaluated using the trapezoidal rule.

VI   RESULTS AND DISCUSSION

The results of the numerical study of heat transfer from an isothermal vertical plate in an air enclosure are presented. Results are presented for the effects of plate location and Grashof number on heat transfer from the plate surface. The investigation was conducted for Pr. No. = 0.72, and heated plate of length, $L_p = (1/3)H$ but negligible width. A maximum Grashof number, Gr. = 4.65E+06, which allows for the stability of the numerical scheme has been employed. This implies a Raleigh number, Ra = 3.35E+06, corresponding to a laminar flow regime.

Figures 2 – 5 present the effects of plate location on the rate of heat transfer from the hot surface. Figures 2 and 5 respectively compare Nusselt numbers at corresponding times for three different horizontal shifts of the plate, while figures 3 and 4 compare same for three vertical shifts of the plate. It would be observed that the curves exhibit collinearity and same slope at very small times for all plate locations. They also exhibit close region of temporal minimum. From Figs 3 and 4 it would be seen that for the vertical shifts of the plate downwards along the mid-length of the cavity from the mid-height, p = H/2, the curves are approximately collinear. This indicates that only little changes occured in the values of heat transfer coefficient. For the plate position, p > H/2 the curve show significant deviation from those for p < H/2 indicating lower values of heat transfer coefficients and therefore lower rates of heat transfer. For a horizontal shift of the plate, figures 2 and 5,

184

the rate of heat transfer decreases as the plate is moved away from the mid-length position towards the left vertical bounding walls after the
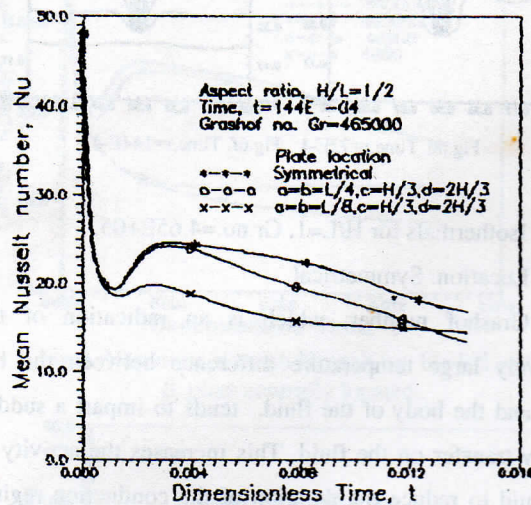

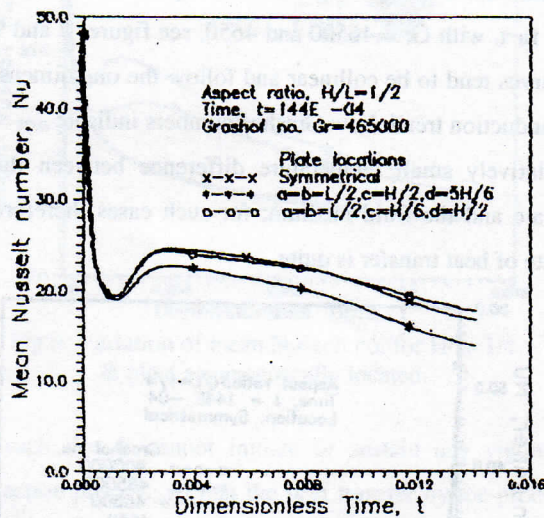Fig.2. Variation of mean Nusselt no. along plate mid-height for H/L=1/2 & Gr.=465000.

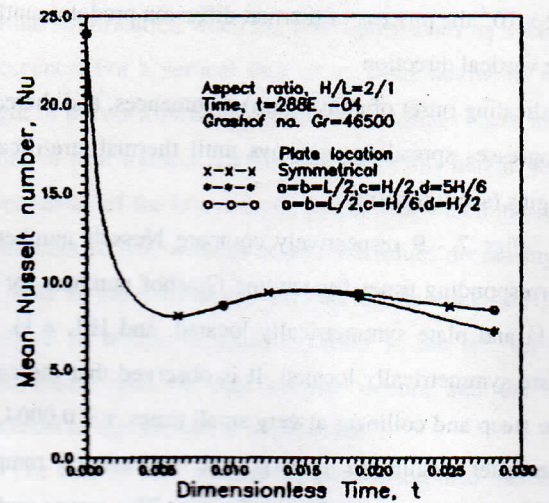Fig.3. Variation of mean Nusselt no. along plate mid-length for H/L=1/2 & Gr. =465000..

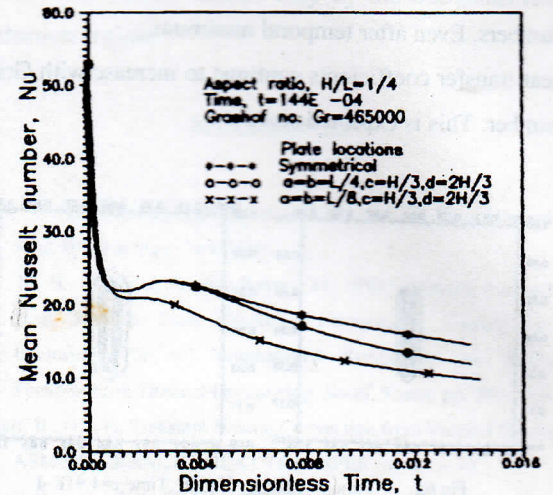Fig.4. Variation of mean Nusselt no. along plate mid-length for H/L=2 & Gr.=46500.

Fig.5. Variation of mean Nusselt no. along plate mid-height for H/L=1/4 & Gr.=463000.

onset of convection. But very close values of the coefficient are observed immediately after the onset of convection for positions $L/4 < a = b \leq L/2$. For plate positions $a = b \leq L/8$ larger deviations in the values of heat transfer coefficient are observed immediately after the common region of temporal minimum.

Figures 6a-f show the process of gradual development of isotherms for H/L = 1, Gr = 465000, and plate symmetrically located. It would be observed from the figures that at small times ($\tau \leq 4.91 \times 10^{-4}$) the isotherms are parallel to the plate surface indicating equal rate of heat transfer in all directions, which is characteristics of conduction heat transfer from an isothermal surface. For $\tau \approx$

185

8.2 x 10^{-4} the process of thermal diffusion predominantly in the vertical direction

(indicating onset of convection) commences, and thereafter progresses spreading sideways until thermal stratification begins (see figure 6f).

Figs 7 - 9 respectively compare Nusselt numbers at corresponding times for varying Grashof numbers for H/L = ¼ and plate symmetrically located, and H/L = ½ and plate symmetrically located. It is observed that the curves are steep and collinear at very small times, τ < 0.0004, and thereafter begins to undergo the process of temporal minimum in heat transfer coefficients. The curves undergo temporal minimum in order of magnitude of Grashof numbers. Even after temporal minimum,

heat transfer coefficients continue to increase with Grashof number. This is expected since a
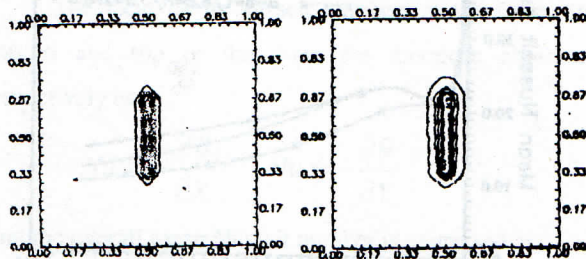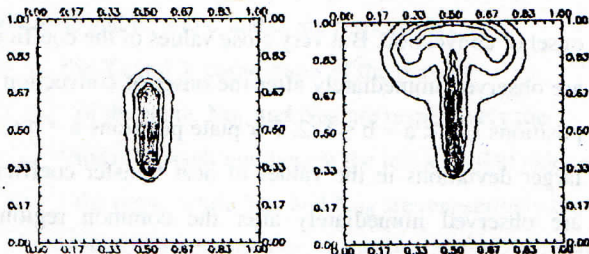

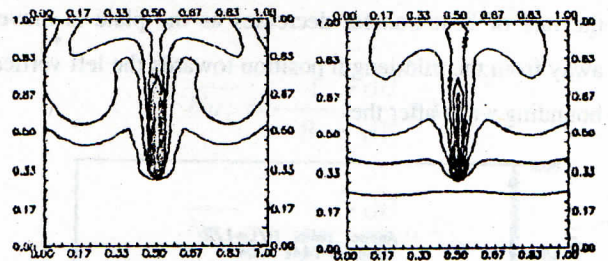Fig.6a.　Time,τ=1.6E-4　Fig.6b. Time,τ=4.91E-4

Fig.6c. Time,τ=8.2E-4　Fig.6d. Time,τ=36E-4

Fig.6e. Time,τ=72E-4　Fig.6f. Time,τ=144E-4

Fig.6. Isothermals for H/L=1, Gr.no.=4.65E+05,
　　　Location: Symmetrical

high Grashof number, which is an indication of the relatively large temperature difference between the hot plate and the body of the fluid, tends to impart a sudden energy transfer on the fluid. This increases the activity of the fluid to reduce the duration of the conduction regime and trigger early convection. The region of temporal minimum is more conspicuous for higher Grashof numbers, in fact, with Gr = 46500 and 4650, see figures 7 and 9, the curves tend to be collinear and follow the one-dimensional conduction trend. Low Grashof numbers indicate

relatively small temperature difference between the hot plate and the fluid medium; for such cases therefore, the rate of heat transfer is quite
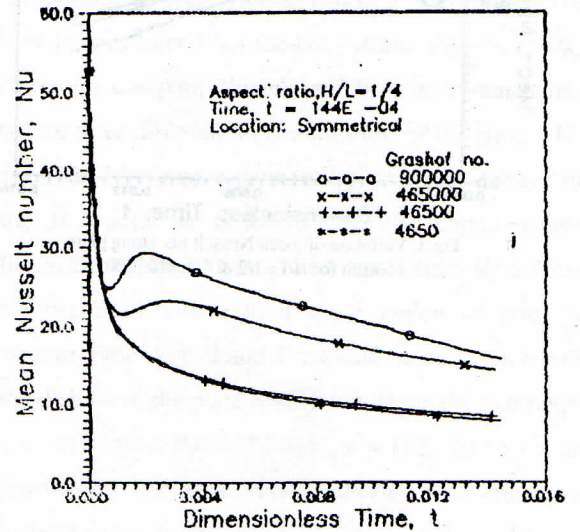

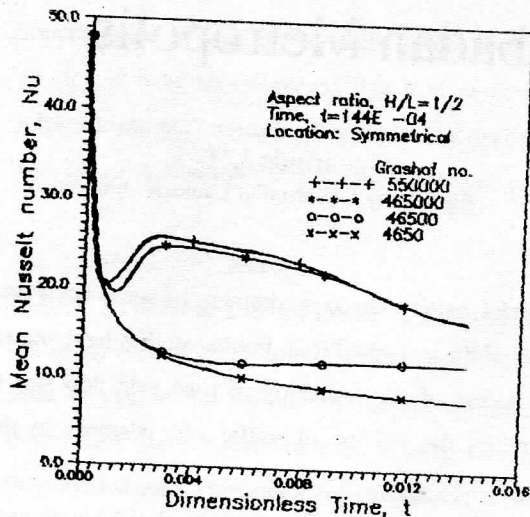Fig.7. Variation of mean Nusselt no. for H/L=1/4
& plate centrally located.

186

Fig.8. Variation of mean Nusselt no. for H/L=1/2
& plate centrally located.
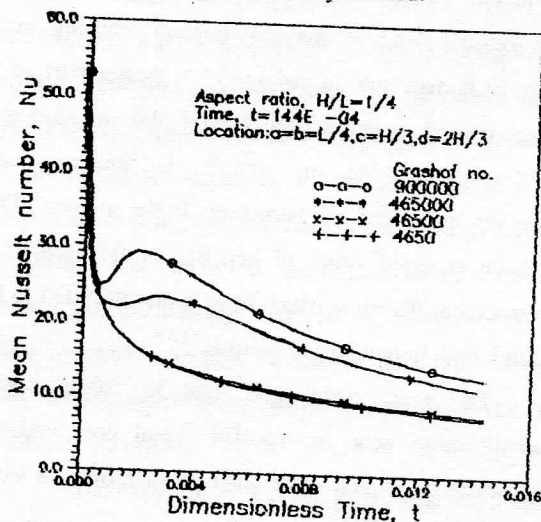

Fig.9. Variation of mean Nusselt no. for H/L=1/4
& plate asymmetrically located.

low such that it cannot initiate or sustain any vigorous convection process; so that the heat transfer by the process resembles that of a one-dimensional conduction regime.

V.   CONCLUSION

In this study it has been demonstrated that in the heat transfer from an isothermal vertical plate in an air enclosure essentially three different regimes of flow are distinguishable: the one-dimensional conduction regime at short times, convection regime at later times, and thereafter thermal stratification when the flow approaches its eventual quiescence. For a vertical shift of the plate below the mid-height of the enclosure only little or no changes occur in the values of heat transfer coefficient Above this height, much lower values of the heat transfer coefficient which indicates lower rates of heat transfer occur, the values decreasing as the plate is moved towards the top of the enclosure. For positions in which the plate is closer to the left vertical walls lower rates of heat transfer occurs and the rate decreases as the left wall is approached.

The rate of heat transfer by convection also increases with Grashof number. Below certain values of the Grashof number heat transfer occurs only by the one-dimensional conduction regime.

REFERENCES

Chow, C. Y., (1979), An Introduction to Computational Fluid Mechanics, John Wiley & Sons, New York.

Eseki, M. H., Reises, J. A., and Behnia, M., (1993), Natural Convection Heat Transfer from Electronic Components Located in an Enclosure, The 6th. International Symposium on Transport Phenomena in Thermal Engineering, Seoul, Korea, pp. 249 – 254.

Gebhart, B., (1961), Transient Natural Convection from Vertical Elements, ASME JOURNAL OF HEAT TRANSFER, pp. 61 – 70.

Gebhart, B., and Adams, D. E., (1962), Measurements of Transient Natural Convection in Flat Vertical Surfaces, ASME JOURNAL OF HEAT TRANSFER, Vol. 83, pp. 1 – 4.

Hellums, J. D., and Churchill, S. W., (1962), Transient and Steady State, Free and Natural Convection, Numerical Simulations: Part 1. The Isothermal Vertical Plate, AIChE Journal, Vol 8, pp. 690 -692.

Khalilolahi A. and Sammakia B. (1986), Unsteady natural Convection Generated by a Heated Surface Within an Enclosure, Numerical Heat Transfer, Vol. 9, pp. 715 – 730.

Ostrach S., (1972) , Natural \convection in Enclosures, Advances in Heat Transfer, Vol. 8, pp. 161 – 227.

Sammakia, B., Gebhart, B., and Qureshi, Z. H., (1980), Measurements and Calculations of Transient Natural Convection in Air, Int. J. Heat and Mass Transfer, Vol. 23, pp. 571 – 576.

Shoichiro, N., (1977), Computational Methods in Engineering and Science, John Wiley & Sons Inc., New York.

187